THE PROMISE OF FIRST SPECTROSCOPY OF NORMAL AND DWARF GALAXIES

J. Fischer

Naval Research Laboratory, Remote Sensing Division, Code 7213, Washington DC 20375, USA

Abstract

ISO spectroscopic studies of galaxies gave us a taste of the diversity of IR spectroscopic signatures of galaxies and their potential to characterize stellar populations and their effects on the local interstellar medium, but also led to ambiguities in interpretation because only the brightest lines were detected in many galaxies. FIRST studies will provide a rich and high signal-to-noise database for understanding the emission line deficit and absorption features in warm, heavily obscured moderate luminosity galaxies like NGC 4418 and in the ultraluminous galaxies. Combined with ground-based, SOFIA and SIRTF studies, FIRST will be able to study starburst evolution in galactic disks, gaseous abundance variations and gradients among Hubble types and the affects of active galactic nuclei on the central regions of these galaxies. Even spectroscopic studies of dusty ellipticals will be possible and will allow us to probe the signatures of heating by old populations and possibly to discover the starburst phenomenon within some of these early-type galaxies. FIRST spectroscopic and broadband studies of low metallicity blue compact dwarf galaxies will provide important templates for interpreting the spectra of luminous galaxies at high redshift. FIRST broadband studies of galaxies with $L_{IR} \sim$ L* will probe out to z $\sim$ 1 while FIR spectroscopy will for the first time be able to fully probe the Hubble sequence of galaxies in the local universe.

Key words: Galaxies: normal – Galaxies: low metallicity – Spectroscopy: far-infrared – Missions: FIRST

1. Introduction

Far-infrared imaging and spectroscopy of galaxies can provide quantitative diagnostics of current star formation processes and, via abundance diagnostics, of the history of star formation, relatively free of the effects of reddening due to dust. In mergers and interacting galaxies, IR spectroscopy is an essential probe of the exciting source, due to the extreme dust column densities present. Far-infrared spectroscopy of normal galaxies is important for several reasons. Even in normal galaxies, the sites of recent star formation are often heavily obscured in the optical. In nearby galaxies, the nuclei and spiral arms can be spatially resolved for studies of the morphology of star formation as a function of Hubble-type. Moreover, normal galaxies provide nearby templates for the understanding of local starburst galaxies and hosts of active galactic nuclei and of more distant high-z galaxies.

In section 2, I review some of the highlights of extragalactic far-infrared and submillimeter imaging and spectroscopic studies carried out with the Infrared Space Observatory (ISO), the Kuiper Airborne Observatory (KAO), and other facilities. I then discuss some of the interesting questions on the evolution of galaxies and speculate on how these issues may be addressed by FIRST studies of normal and dwarf galaxies in section 3.

2. Recent FIR spectroscopic and imaging results

2.1. Full ISO FIR spectra of IR-bright galaxies

Our ISO Long Wavelength Spectrometer (LWS) central program study of a small sample of IR-bright galaxies (Fischer et al. 1999; Fischer et al. 2001a) demonstrates the richness of this spectral range and the variety of spectra we can expect to obtain of normal galaxies with the higher sensitivity of FIRST. Figure 1 shows our sequence of full, high signal-to-noise LWS spectra of six infrared bright galaxies in order of the relative strength of the [O III] 52, 88 μm fine-structure lines. The spectral sequence extends from the strong emission line galaxies Arp 299 (Satyapal et al. 2001a) and M 82 (Colbert et al. 1999) to the ultraluminous galaxy (ULIG) Arp 220 (Fischer et al. 2001a,b), whose spectrum is dominated by absorption lines of OH, H_2O, CH, and [O I], with only very weak [C II] 158 μm and OH 163 μm line emission. Intermediate in the sequence are Cen A (Unger et al. 2000), NGC 253 (Bradford et al. 1999; Bradford et al. 2001) and NGC 4945 (Lord et al. 2001), showing weak [O III] and [N III] lines while their PDR emission lines remain moderately strong. In this sequence, the strength and richness of the molecular absorption spectra are anti-correlated with the equivalent widths of the fine-structure emission lines. For example, M 82 shows faint OH absorption from the ground level at 119 μm, while NGC 253 shows absorption from the ground-state in three cross-ladder transitions and an emission line cascade in the 79 μm and 163 μm lines. In Arp 220, absorption from rotational levels as high as 416 K and

Proc. Symposium *'The Promise of the Herschel Space Observatory'* 12–15 December 2000, Toledo, Spain
ESA SP-460, July 2001, eds. G.L. Pilbratt, J. Cernicharo, A.M. Heras, T. Prusti, & R. Harris

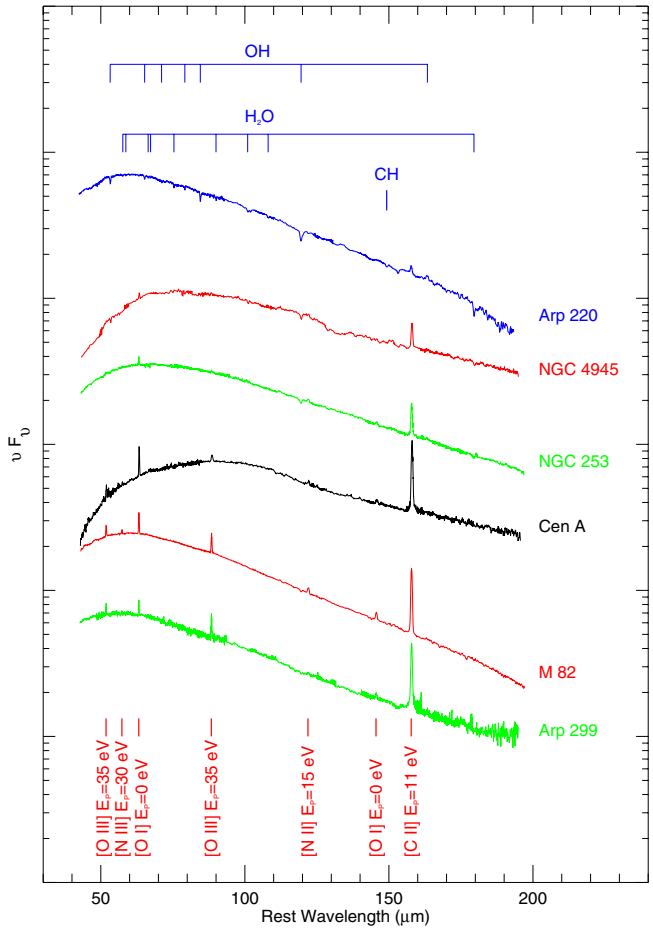

Figure 1. The full ISO Long Wavelength Spectrometer spectra of six IR-bright galaxies. The spectra have been shifted and ordered vertically according to the equivalent width of the [O III]88 μm line. The excitation potential, the energy required to create the species, is given in eV at the bottom of the figure. From Fischer et al. (1999).

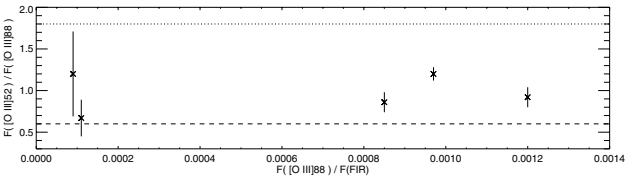

Figure 2. The [O III]52 μm/[O III]88 μm line ratio versus the [O III]88 μm line to integrated far-infrared continuum flux ratio for the sample galaxies. The dashed and dotted lines show the [O III] line ratio in the low density limit (≤ 100 cm^{-3}) and for an electron density of 500 cm^{-3}, respectively (Fischer et al. 1999).

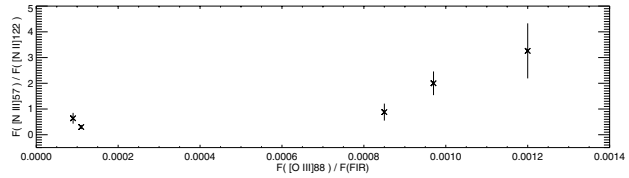

Figure 3. As in Figure 2 for the [N III]57 μm/[N II]122 μm line ratio.

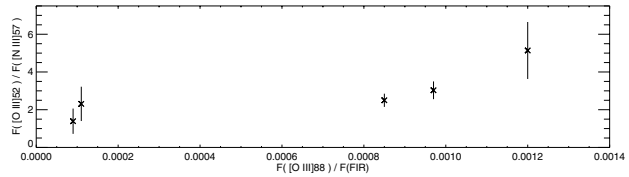

Figure 4. As in Figure 2 for the [O III]52 μm/[N III]57 μm line ratio.

305 K above the ground state is present for OH and H_2O respectively, and the [O I]63 μm line is seen in absorption.

Population synthesis and photoionization models of dusty, infrared-bright galaxies such as Arp 299, M 82, and NGC 4038/39, indicate that short-lived bursts of star formation with ages of 3-7 × 10^6 years, can explain the spectra of these galaxies (Satyapal et al. 2001a, Colbert et al. 1999, and Fischer et al. 1996). Thornley et al. (2000) find similar results from an analysis of their [Ne III]15.6 μm, [Ne II] 12.8 μm survey of 27 starburst galaxies. Satyapal et al. show that the models derived from LWS measurements including all of the individual components of Arp 299 are indeed consistent with the ensemble of model fits to high spatial resolution Brackett γ images of individual components of this galaxy. Unger et al. (2000) find that in Cen A as well, the extended far-infrared emission appears to be powered primarily by star formation rather than by the central obscured AGN.

Using the temperature-insensitive [O III]52/[O III]88 line ratio as a probe of density (fig 2), Fischer et al. (1999, 2001a) find no clear dependence of the [O III]88/F_{FIR} ratio on electron density and all of the measured [O III] line ratios fall within the range 0.6 - 1.2, consistent with electron densities between 100 - 500 cm^{-3}. From this they infer that neither density nor far-infrared differential extinction (between 52 - 88 μm) to the ionized gas appears to be the single dominant parameter in the observed sequence. Rather, since both of the line ratios [N III]57 to [N II]122 (fig 3) and [O III]52 to [N III]57 (fig 4) increase as a function of the [O III]88/F_{FIR} ratio, they infer that [O III]88/F_{FIR} correlates with excitation. They suggest that the effects of absorption by dust in ionized regions with high ionization parameters may explain these effects and that the OH and H_2O molecules producing the FIR absorption lines in ULIGs such as Arp 220 and Mkn 231 (Harvey et al. 1999) may be located in dense photodissociation regions, where they could be excited radiatively by the far-infrared emission from warm dust. If extinction plays a role in this sequence it appears from this analysis that the affected regions are very heavily obscured even in the far-infrared, while the detected line emission is relatively unobscured. In this case, the progression to

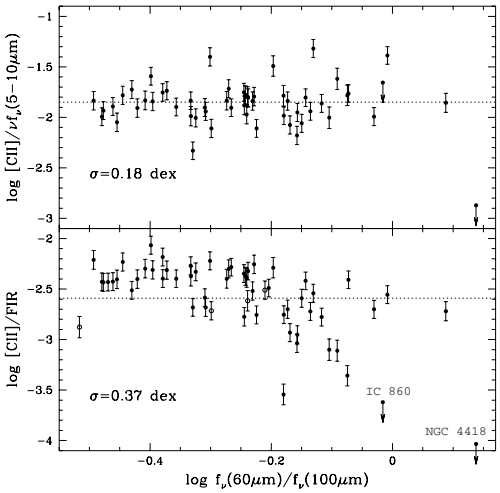

Figure 5. The ratio of the [C II] line to the ISOCAM LW2 5 - 10 μm band flux (a tracer of PAH emission) is found to be constant for the ISO normal galaxies key program sample (Helou et al. 2001, top) in contrast to the ratio [C II]/FIR (bottom) which declines for galaxies with higher IRAS FIR color (Malhotra et al. 1997, 2001). The empty circle symbols are early-type galaxies discussed by Malhotra et al. (2000). Adapted from Helou et al. (2001).

low excitation could be a result of total obscuration of the central AGN and/or the youngest starburst population.

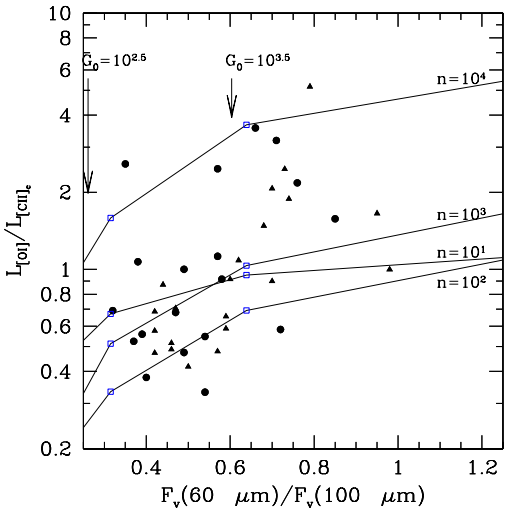

Figure 6. The [O I]63 μm/[CII]$_C$ luminosity ratio plotted against the ratio of the fluxes in the IRAS 60 μm and 100 μm bands for galaxies from the ISO normal galaxies key program compared with PDR model predictions for a range of n and G_o (Malhotra et al. 2001). Here Malhotra et al. have subtracted a contribution to the [C II] luminosity from ionized gas based on a scaling relation from the observed [N II] line luminosity (circles represent galaxies with detected [N II] and triangles represent galaxies where a 2σ upper limit was used). From Malhotra et al. (2001).

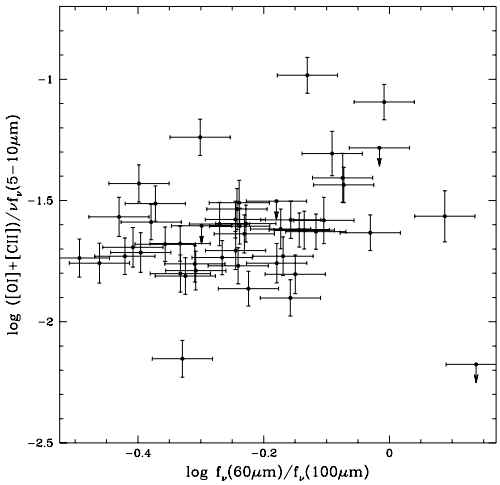

Figure 7. As in the lower panel of Figure 5 for the ratio of ([C II] + [O I]) to the ISOCAM LW2 5 - 10 μm filter flux. ([C II] + [O I])/PAH increases with FIR color temperature in contrast to [C II]/PAH, which stays constant. Note the lowest ratio plotted is for NGC 4418, whose LW2 flux is dominated by continuum (Lu et al. 2001). From Helou et al. (2001).

2.2. Spectroscopic studies of PDRs in galaxies

Additional understanding of the obscured sources of excitation in dusty galaxies can be obtained from statistical and imaging studies of the strong FIR fine-structure lines and MIR aromatic feature emission from photodissociation regions (PDRs) that surround the ionized gas around young stars.

In analyses of the ISO normal galaxies key program data, Malhotra et al. (1997, 2001) found that as the FIR color temperature and L_{FIR}/L_{Blue} ratio of a galaxy increase, the [C II]158μ/FIR and the [C II]158μ/[O I]63μ ratios decrease (Figure 5, bottom; see Sanders & Mirabel 1996 for a review of FIR definitions). Using $F_{60\mu}/F_{100\mu}$ and F_{FIR}/F_B as measures of the dust heating radiation density and star formation activity respectively, they argue that these inverse correlations are evidence that low values of [C II]/FIR can be attributed to lower gas heating efficiency due to positively charged grains arising from high values of $\langle G_o \rangle / n$, where G_o is the FUV radiation flux and n is the density. After correcting the observed [C II] fluxes for a contribution from diffuse ionized gas based on [N II] line fluxes (Figure 6) they are able to fit the data with the PDR models of Kaufman et al. (1999). In early-type galaxies however, low values of [C II]/FIR are attributed to the relative softness of the radiation field (Malhotra et al. 2000), while in blue compact dwarfs, the [C II]158 μm and other fine-structure lines are strong (Madden 2000; 2001).

In contrast to the low [C II]/FIR (as well as low ([C II] + [O I])/FIR) at high FIR color temperatures, the ratio of the [C II] line flux to the ISOCAM LW2 (5 - 10 μm) band flux, a tracer of polycyclic aromatic hydrocarbon

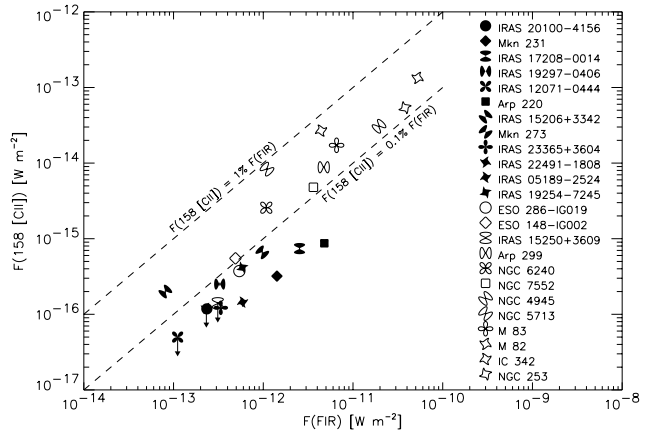

Figure 8. The [C II]158 μm line flux versus FIR flux for 12 ULIGs observed with the LWS (Luhman et al. 1998; 2001) compared with a sample of normal and starburst galaxies (Luhman et al. 1998; Lord et al. 1996; Colbert et al. 1999; Stacey et al. 1999; Bradford et al. 1999). In the symbol key, the galaxies are listed in order of luminosity from top to bottom and the ULIG symbols are black filled, while the lower luminosity galaxies are unfilled. ULIGs are defined as in Sanders & Mirabel (1996). The dashed lines mark the regime typical of normal and starburst galaxies. From Luhman et al. (2001).

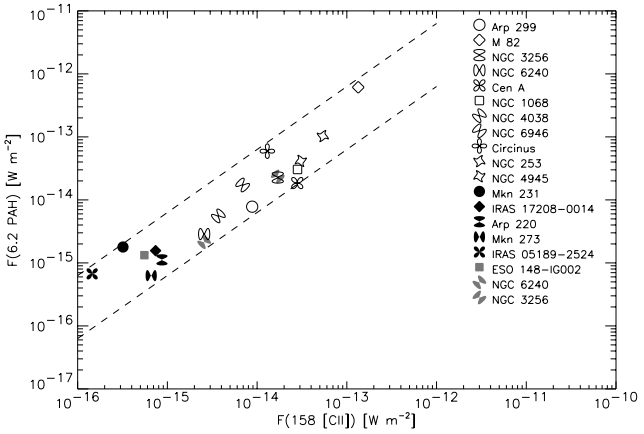

Figure 9. The 6.2 μm PAH feature versus [C II]158 μm line flux for ULIGs and other IR-bright galaxies. The 6.2 μm PAH emission was measured from CAM CVF spectra (open symbols), integrated over the full LWS beam for galaxies with extended emission, and from PHOT-S spectra (filled symbols) for compact galaxies (Dudley et al. 2001). Black, filled symbols are ULIGs, while unfilled or grey filled symbols are lower luminosity galaxies. Dashed lines show a range of a factor of 10 in the flux ratio. From Luhman et al. (2001).

feature emission (PAH), is constant (Helou et al. 2001, Figure 5, top)! As Helou et al. (2001) point out, the increase of ([C II] + [O I])/PAH with color temperature (see Figure 7) points to the increased importance of non-PAH grain populations or to emission contributions from components with very different physical conditions.

Whereas most normal and lower luminosity starburst galaxies have [C II]/FIR ratios between 10^{-2} - 10^{-3}, this ratio is about an order of magnitude lower in ULIGs (Luhman et al. 1998, 2001; Figure 8). In contrast, and consistent with the results of Helou et al. (2001) for normal galaxies, Luhman et al. (2001) have found that the average value and spread of the [C II] 158 μm line to 6.2 μm PAH feature intensity ratio is similar in ULIGs and other IR-bright galaxies (Figure 9). The 6.2 μm feature is an isolated feature, well separated from other narrow PAH features and the 9.8 μm silicate absorption feature and was measured from CAM CVF spectra, integrated over the full LWS beam for galaxies with extended emission, and from PHOT-S spectra for compact galaxies. Luhman et al. (2001) reason that high $\langle G_o \rangle / n$ conditions causing low values of the [C II]/FIR ratio, would not produce correspondingly low values of the 6.2 μm/FIR ratio, unless a significant fraction of the grains responsible for the 6.2 μm feature are destroyed by these conditions. However, laboratory studies indicate that PAH sizes greater than 50 C-atoms probably dominate the emission in this band (Hudgins & Allamandola 1999) while theoretical studies indicate that it is difficult to destroy PAHs with greater than 50 C-atoms in the regimes of $\langle G_o \rangle / n$ thought to exist in these galaxies (Allain et al. 1996; A. Tielens, private communication) unless the radiation spectrum is harder. Thus these observations suggest that properties such as the average differential extinction to and the average photoelectric heating efficiency in *the starburst regions* in ULIGs and starburst galaxies may be similar. Luhman et al. (2001) find evidence for differing filling factors among PDR line diagnostics of [C II], [C I], and CO(1-0) and warn that when using the method developed by Wolfire et al. (1989) the results must be checked for consistency. They suggest that additional dusty components of FIR emission may be present, possibly associated with very high ionization parameters (Satyapal et al. 2001b; Fischer et al. 2001a) and/or hidden AGN (Dudley et al. 2001), as has also been suggested for the very low [C II]/FIR, highly obscured galaxy NGC 4418 (Spoon et al. 2001). It is important to note that while Genzel et al. (1998) use low PAH feature equivalent width as an indicator of the presence of an AGN, Clavel et al. (2000) find that although the mean equivalent width in the Seyfert 1 galaxies in their study is a factor of 5.4 lower than that of their Seyfert 2 counterparts, the mean PAH *luminosities* of the two types are equal. They attribute the high mean equivalent width in Seyfert 2's to extinction of the hot dust continuum. If this is true, then the PAH/FIR flux ratio and possibly the [C II]/FIR ratio, may better diagnostics of the contribution of AGN to the FIR luminosity than the PAH equivalent width.

Applying PDR models to their [C I] submillimeter observations of nearby galaxies in comparison with [C II] and CO lines, Gerin & Phillips 2000 find that the ULIGs

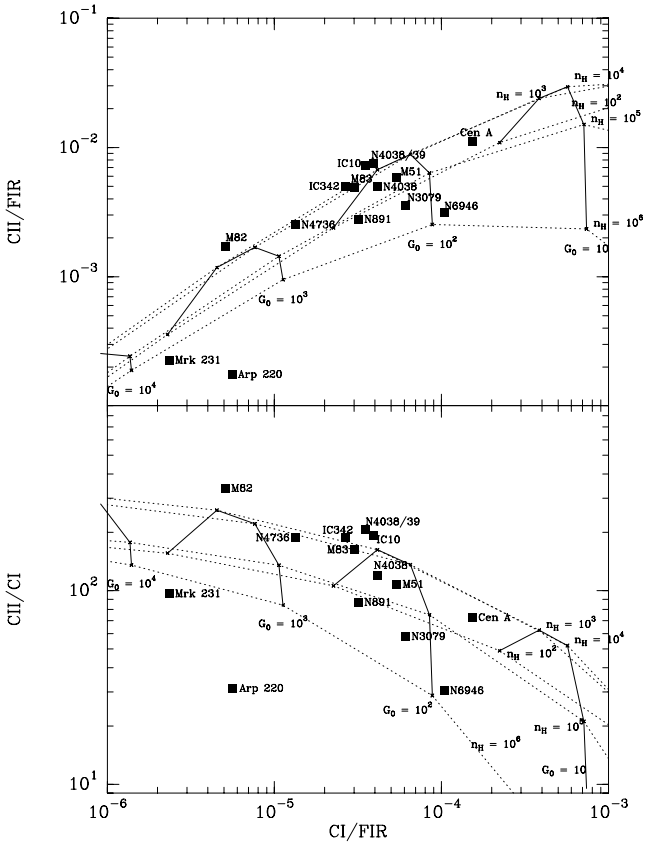

Figure 10. The [CII] to far-infrared flux ratio (top) and [C II]/[C I] line ratio (bottom) versus [C I]/FIR in a 55″ beam. The lines show PDR model predictions for $n_H = 10^2$ - 10^6 cm^3 and $G_o = 10$ - 10^4. The solid lines are for constant G_o; the dashed lines are for constant density. The location of the two ULIGs Arp 220 and Mkn 231 are below the predictions of current PDR models even for high G_o and high n_H. From Gerin & Phillips (2000).

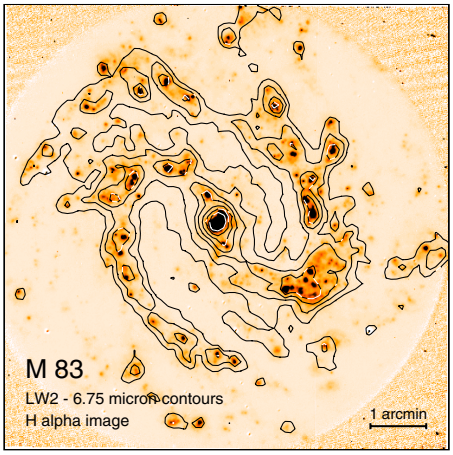

Figure 11. ISOCAM LW2 6.75 μm contours, superposed on an Hα image of M 83. The images are well correlated, showing that the aromatic feature (PAH) emission traced by the LW2 filter is associated with star forming regions and a good tracer of PDR emission. From Vogler et al. (2001).

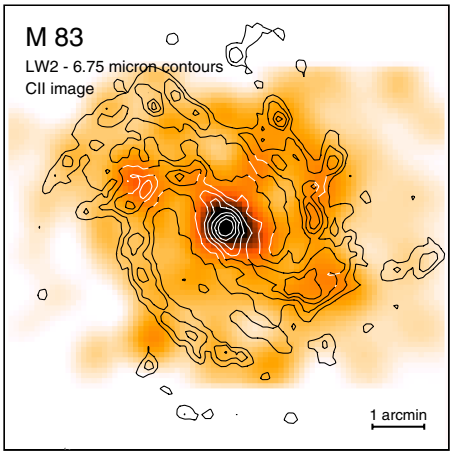

Figure 12. Here the LW2 6.75 μm contours are superposed on a [C II] 158 μm line intensity map of M 83 obtained with FIFI on the Kuiper Airborne Observatory (55″ resolution). Despite the low resolution of the FIFI images, they show correlation of [C II] with star forming regions. PACS will provide images of [C II] emission in nearby galaxies with resolution comparable to the ISOCAM LW2 images. From Vogler et al. (2001).

Arp 220 and Mkn 231 lie below the predictions of current PDR models even for high G_o and high n, and suggest that both line and continuum optical depth effects may play a role in the [C II] deficit in ULIGs. Detailed studies of many diagnostic lines in larger samples with FIRST and other missions will further our understanding of the physical effects at work in these galaxies. Successful models will need to provide understanding of the relative lines strengths and weakness of all of the IR - submillimeter lines in high FIR color temperature and often very luminous galaxies.

2.3. IR imaging spectroscopy of normal galaxies

ISOCAM imaging studies of nearby galaxies provide further evidence that [C II] in galaxies is associated with star forming regions. Vogler et al. (2001) find that LW2 band images that trace PAH emission are well correlated with both Hα (Figure 11) and [C II] (Figure 12) images obtained with the FIFI instrument obtained with the NASA Kuiper Airborne Observatory (KAO). FIRST will provide FIR spectroscopic images with resolution comparable to these mid-IR images and will thus allow FIR imaging spectroscopy of halo, spiral arm, interarm, and extended disk emission above and below the planes (eg. Madden et al. 1993) of nearby galaxies. Through coordinated studies with other observatories, FIRST spectroscopy can contribute to the measurement of interstellar abundance variations in disks of nearby galaxies, similar to that carried out for the Milky Way by Simpson et al. (1995). Our own galactic center is characterized by about a factor of three

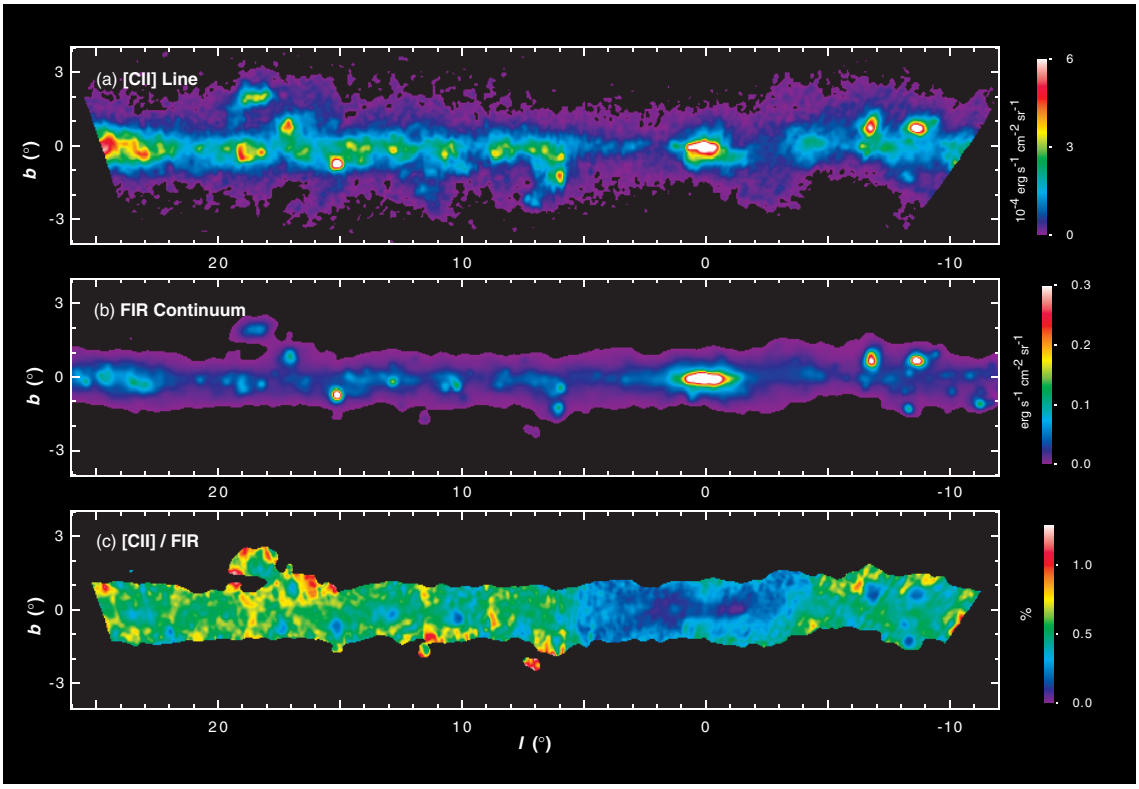

Figure 13. (a) [CII]158 μm line intensity map of the galactic center and the surrounding galactic plane obtained by the Balloon-borne Infrared Carbon Explorer (BICE). (b) Far-infrared offset-subtracted continuum map obtained from IRAS 60 μm and 100 μm data smoothed to 15′ the resolution of the BICE [C II] map. (c) The [C II]/FIR ratio. From Nakagawa et al. (1998).

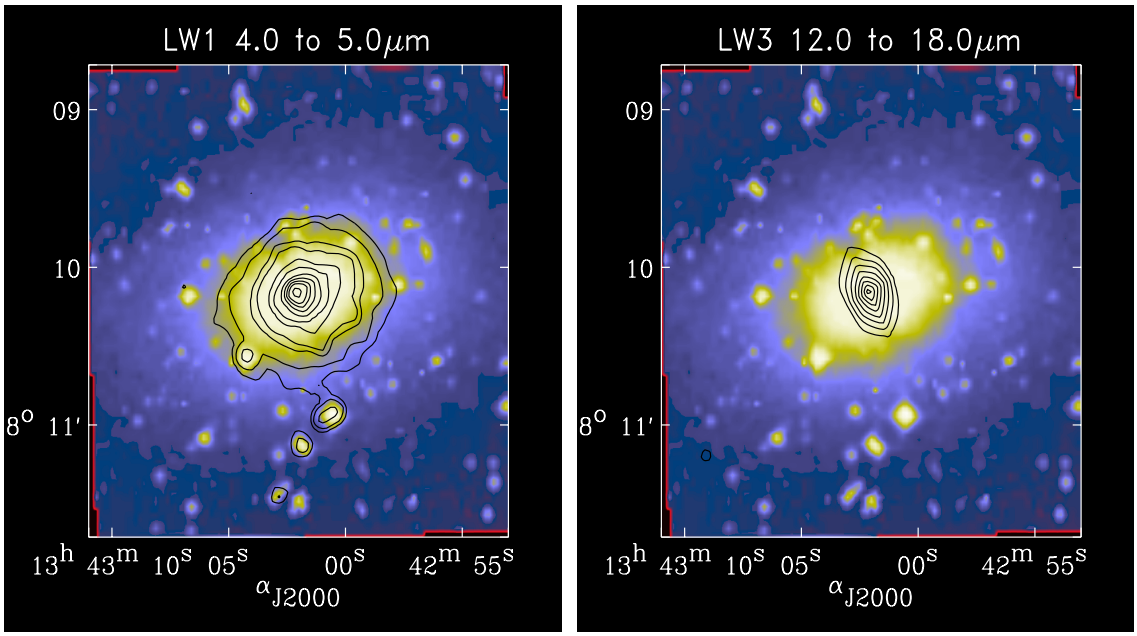

Figure 14. ISOCAM LW1 4 - 5 μm (left contours) and LW3 12 - 18 μm (right contours) images of the early type galaxy NGC 5266 superposed on an optical image. The LW1 image closely follows the optical image and thus traces the stellar continuum, while the LW3 image is confined to the region of the dust lane. From Madden et al. (1999).

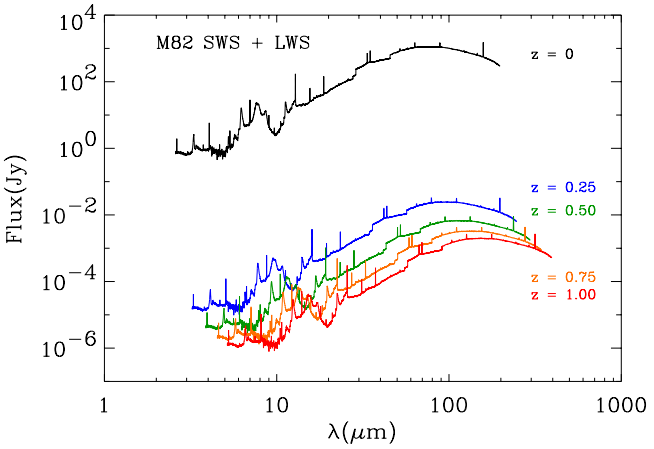

Figure 15. The ISO SWS + LWS spectrum of the infrared-bright galaxy M 82 ($L_{IR} \sim 4 \times 10^{10} L_{\odot}$, Colbert et al. 1999; Sturm et al. 2000) in Janskies and simulated for redshifts between z = 0 - 1, for $H_0 = 75$, $\Omega(0) = 1$, and $\Omega(1) = 0$. The discontinuities in the spectrum and the relative apparent line strengths are artifacts of the specific SWS and LWS instrument apertures and resolving powers. Assuming that in broad-band mode ($R \sim 3$) PACS will measure a few milli-janskies at 10σ in 10 hours, FIRST will be able to measure the broad-band FIR emission of such IR-bright $\sim$ 2 L galaxies for $z < 1$ for the adopted cosmology.*

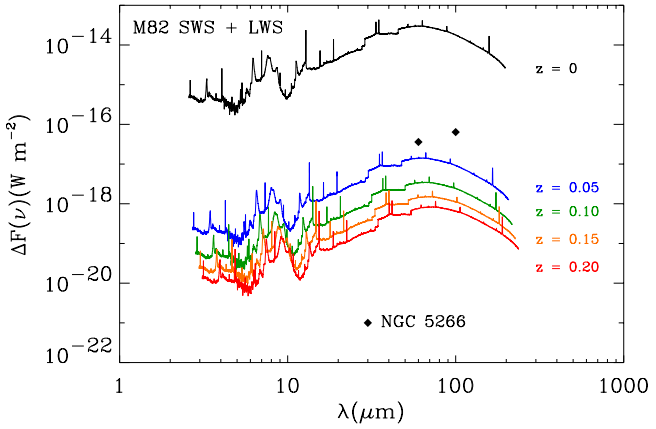

Figure 16. The ISO SWS + LWS spectrum of the infrared-bright galaxy M 82 in W m^{-2} for R = 1700 and simulated for redshifts between z = 0 - 0.2, (see caption for Fig 15). Assuming that in spectroscopic mode PACS will measure 10^{-18} W m^{-2} at 10σ in 10 hours, FIRST will be able to measure the FIR spectra of such IR-bright $\sim$ 2 L galaxies at the peak of their emission for $z < 0.2$, even at line-to-continuum values near unity, for the adopted cosmology. The IRAS 60 μm and 100 μm flux densities of the early type galaxy NGC 5266 (see Fig 14) are also plotted for reference.*

lower [C II]/FIR ratio than is found in more diffuse regions of the galactic plane (Nakagawa et al. 1998; see Figure 13) even for low values of $F_{60\mu}/F_{100\mu}$. Although the reason for this is controversial, the effect of molecular self-shielding is generally acknowledged to play a role (Bennett et al. 1994; Nakagawa et al. 1995). The increased sensitivity and spatial resolution of FIRST over KAO and ISO instruments will allow FIR diagnostic studies of the nuclear regions of nearby galaxies that will help probe the physical conditions in these often highly obscured regions. Even FIR imaging spectroscopy of nearby early-type galaxies will be possible. For example, Figure 14 (Madden et al. 1999) shows contour plots of the MIR emission in the early-type galaxy NGC 5266 in the ISOCAM LW1 4 - 5 μm and LW3 12 - 18 μm bands. The IRAS 60 and 100 μm fluxes measured for this galaxy, presumably associated with the dust lane emission seen in the LW3 image, are bright enough for this galaxy to be studied by PACS in imaging spectroscopic mode (see section 3).

3. FIRST studies of normal and dwarf galaxies

ISO spectroscopy of galaxies gave us a taste of the power of IR spectroscopic diagnostics but also led to ambiguities of interpretation because only the brightest lines were detected in many galaxies. FIRST spectroscopy of nearby normal and dwarf galaxies will provide high signal-to-noise spatially resolved spectra that will help understand conditions in dusty regions of galaxies and help interpret the signatures of high-z galaxies. FIRST broadband studies of normal galaxies will probe out to z $\sim$ 1 and FIR spectroscopy will for the first time be able to probe the Hubble sequence of normal galaxies in the local universe (see Figures 15 and 16).

Hierarchical theories of galaxy evolution are currently the most accepted theories of structure and galaxy formation (eg. Kaufmann et al. 1999 and Cole et al. 2000). These theories hold that galaxies formed from baryonic matter that accumulated in the gravitational potential wells of collapsed cold dark matter halos that grew out of primordial density fluctuations during the inflationary period of the universe. The subsequent growth and evolution of these seed galaxies from late to early type is strongly affected by the high rate of mergers in the past, with ensuing elliptical disk formation.

Recent non-linear analysis has shown that the presence of non-axisymmetric patterns such as spirals or bars may also play a role in galaxy evolution and should be considered as well (Zhang 1999). The presence of these patterns leads to inflow within and outflow outside of the co-rotation point, growth of the bulge, heating of the disk stars, and thus to accelerated morphological evolution of galaxies along the Hubble sequence. Combined with ground-based, SOFIA and SIRTF studies, FIRST will be able to study starburst evolution in galactic disks, gaseous abundance variations and gradients among Hubble types and variations in the heating and cooling mechanisms in the galactic center regions of these galaxies. Even spectroscopic studies of dusty ellipticals will be possible and will allow us to probe the signatures of heating by old populations and possibly to discover the starburst phenomenon

within some of these early type galaxies. Moreover, FIRST spectroscopic and broadband studies of low metallicity blue compact dwarf galaxies will be important templates for interpreting the results of luminous galaxies at high redshift. Madden (2001) and Fritz et al. (2001) present detailed discussions of FIRST studies of low metallicity dwarf galaxies, while Malhotra (2001) discusses FIRST [C II] studies of primeval galaxies, elsewhere in this volume.

Whatever the evolutionary history of galaxies, kinematic studies show that the masses of central massive dark objects, are tightly correlated with the spheroid velocity dispersions (eg. Gebhardt et al. 2000). This tight correlation suggests a causal connection between the formation and evolution of the massive black holes and galaxy bulges. It is natural to assume that bulges, black holes, and quasars formed, grew or turned on as parts of the same process. Further understanding of the IR emission line deficits and absorption features in galaxies like NGC 4418 and the ultraluminous galaxies, through both observational and modeling studies, may ultimately uncover a FIR signature of buried or quenched AGN in the centers of galaxies. Such signatures could provide large galaxy surveys with a means to measure the buried AGN statistics in normal galaxy centers and to study the evolution of central black holes and the evolution of bulges along the Hubble sequence.

Acknowledgements

I would like to thank my collaborators on the LWS IR-bright galaxies team, S. Satyapal, M. Luhman, C. Dudley, M. Wolfire, C. M. Bradford, J. Brauher, P. Cernicharo, P. E. Clegg, J. Colbert, P. Cox, E. Gonzalez-Alfonso, V. Harvey, S. Lord, M. Malkan, G. Melnick, H. A. Smith, L. Spinoglio, G. Stacey, and S. Unger, for their contributions to the work reviewed here, some still in press or in preparation. Thanks also to S. Madden, A. Vogler, G. Helou, and S. Malhotra for access to preprint material before publication, to E. Dwek for use of his program to produce sensitivity plots, and to X. Zhang for helpful discussions. This work was supported by the Office of Naval Research and the NASA Long Term Space Astrophysics program.

References

Allain, T., Leach, S., Sedlmayr, E. et al., 1996, A&A 305, 616
Bennett, C. L., Fixsen, D. J., Hinshaw, G., et al., 1994, ApJ 434, 587
Bradford, C. M., Stacey, G. J., Fischer, J., Smith, H. A., et al., 1999, in *The Universe As Seen by ISO*, eds. P. Cox, M. F. Kessler, ESA SP-427, 861
Bradford, C. M. et al. (2001), in prep.
Clavel, J., Schultz, B., Altieri, B., et al. 2000, A&A, 357, 839
Colbert, J. W., Malkan, M. A., Clegg, P. E., et al., 1999, ApJ 511, 721
Cole, S., Lacey, C. G., Baugh, C. M., Frenk, C. S., 2000, MNRAS, 319, 168
Dudley, C. C., et al. 2001, in prep.
Fischer, J., Shier, L. M., Luhman, M. L., Satyapal, S. et al., 1996, A&A 315, L97
Fischer, J., Luhman, M. L., Satyapal, S. et al., 1999, eds. Lutz, D., Tacconi, L., Astronomy & Space Sci., 266, 91
Fischer, J., et al., 2001a, in prep.
Fischer, J., et al., 2001b, in prep.
Fritz, T., et al., 2001, this volume
Gebhardt, K., et al., 2000, ApJ, 539L, 13
Genzel, R., Lutz, D., Sturm, E., et al., 1998, ApJ 498, 579
Gerin, M., Phillips, T.G., 2000, ApJ, 537, 644
Harvey, V. I., Satyapal, S., Luhman, M. L., Fischer, J., et al., 1999, in *The Universe As Seen by ISO*, eds. P. Cox, M. F. Kessler, ESA SP-427, 889
Helou, G, Malhotra, S., Hollenbach, D. J., Dale, D. A., Contoursi, A. et al., 2001, ApJ, in press
Hudgins, D. M., Allamandola, L. J., 1999, ApJ 513, L69
Kaufman, M. J., Wolfire, M. G., Hollenbach, D., Luhman, M. L., 1999, ApJ 527, 795
Kauffmann, G., Charlot, S., Haehnelt, M., 2000, MNRAS, 311, 576
Lord, S. D., Malhotra, S., Lim, T., 1996, A&A 315, L117
Lord, S. D., et al., 2001, in prep.
Luhman, M. L., Satyapal, S., Fischer, J., Wolfire, M. G., et al., 1998, ApJ 504, L11
Luhman, M. L. et al., 2001, in prep.
Lu, N. et al., 2001, in prep.
Madden, S. C., Geis, N., Genzel, R., et al., 1993, ApJ, 407, 579
Madden, S. C., Vigroux, L., Sauvage, M., 1999, in *The Universe As Seen by ISO*, eds. P. Cox, M. Kessler, ESA SP-427, 933
Madden, S. C., 2000, in New Astronomy Reviews, *The Interplay between Massive Stars & the ISM*, eds. D. Schaerer, R. Delgado-Gonzalez, 44, 249
Madden, S., 2001, this volume
Malhotra, S., Helou, G., Hollenbach, D., Lord, S., et. al., 1997, ApJ, 491, L27
Malhotra, S., Hollenbach, D., Helou, G., et. al., 2000, ApJ, 543, 634
Malhotra, S., Kaufman, M., Hollenbach, D., Helou, G., et. al., 2001, ApJ, submitted
Malhotra, S., 2001, this volume
Nakagawa, T., Yui, Y., Doi, Y. et al., 1998, ApJS 115, 259
Nakagawa, T., Doi, Y., Yui, Y. Y., et al., 1995, ApJ, 455, L35
Sanders, D. B., Mirabel, I. F., 1996, ARAA 34, 749
Satyapal, S., Luhman, M. L., Fischer, J., Wolfire, M. G. et al., 2001a, ApJ, submitted
Satyapal, S. et al., 2001b, in prep.
Simpson, J., Colgan, S., Rubin, R., Erickson, E., Haas, M., 1995, ApJ, 444, 721
Spoon, H. W. W., Keane, J. V., Tielens, A. G. G. M., Lutz, D., Moorwood, A. F. M., et al., 2001, A&A, 265, 353
Stacey, G. J., Swain, M. R., Bradford, C. M., Barlow, M. J. et al., 1999, in *The Universe As Seen by ISO*, eds. P. Cox, M. F. Kessler, ESA SP-427, 973
Thornley, M. D., Forster-Schreiber, N. M., Lutz, D., Genzel, R., et al., 2000, ApJ, in press
Unger, S.J., Clegg, P., Stacey, G., et al., 2000, A&A, 355, 885
Vogler, A., Madden, S. et al., 2001, in prep.
Wolfire, M. G., Hollenbach, D., Tielens, A. G. G. M., 1989, ApJ, 344, 770
Zhang, X., 1999, ApJ, 518, 613